

Characterization of the transport properties of MoO₃ films on copper

C. Bonavolontà¹⁾, M. Valentino^{1,2)}, M. de Lucia¹⁾, M. Ambrosio¹⁾,
C. Aramo¹⁾, S. Macis³⁾, I. Davoli³⁾, G. Castorina^{4,5)}, F. Monforte⁶⁾,
B. Spataro⁴⁾, M. Scarselli³⁾, S. Lupi⁷⁾ and A. Marcelli^{4,8)}

¹⁾ *INFN, Sezione di Napoli, Via Cintia 2, 80126 Napoli, Italy*

²⁾ *CNR-ISASI via Campi Flegrei 34, 80078 Pozzuoli (Napoli), Italy*

³⁾ *Università di Tor Vergata, Via della Ricerca Scientifica 1,
00133 Roma, Italy*

⁴⁾ *INFN - Laboratori Nazionali di Frascati, P.O. Box 13, 00044, Frascati, Italy*

⁵⁾ *University of Catania, Dipartimento di Ingegneria Elettrica,
Elettronica e Informatica, 95126 Catania, Italy*

⁶⁾ *CNR, Istituto per la Microelettronica e Microsistemi- IMM, VIII Strada 5,
95121 Catania, Italy*

⁷⁾ *INFN and Department of Physics, University of Rome La Sapienza,
P.le A. Moro 2, 00185, Rome, Italy*

⁸⁾ *RICMASS, Rome International Center for Materials Science Superstripes,
00185 Rome, Italy*

Abstract

In this study we report the first transport experiments performed on a series of thin films of MoO₃ grown on a thick Cu substrate. Electrical resistance measurements have been performed for different film thickness as function of temperature down to ~20 K. Data show, due to the copper substrate, that thin films of molybdenum trioxide also at low temperature exhibits a metallic behaviour while for films with a thickness > 250 nm the semiconducting behaviour start to prevail on the metallic one. Local morphological properties and optical data are also showed to support the interpretation of the conductive behaviour of these thin layers of molybdenum oxides.

1 Introduction

Thin films coated on a substrate may control and improve some properties of the substrate. However, in the literature few studies are devoted to the characterization of metallic coatings on a metallic substrate. A recent work deals with the case of TM oxides grown on transition metals, in particular Mo and Cu (TM) oxides on copper [1]. Taking into account the complex molybdenum oxide phase diagram, the most interesting combination is represented by MoO_3 on copper. Indeed, due to its properties a thin "insulating" layer of MoO_3 deposited on a thick copper substrate tends to become conductive, while its work function should remain high and constant (~ 7 eV). This result is fully in agreement with a study recently published at BESSY that reported the decrease of the Field Effect from an oxidized surface where has been observed the formation of islands of MoO_3 [2]. Following previous characterizations of molybdenum films [3,4], here we present preliminary studies of MoO_3 layers of different thickness on a Cu substrate at room temperature and a study of transport properties vs. temperature down to ~ 20 K.

2 Material preparation

For the preparation of the thin films we first polished and cleaned the copper substrate and after we evaporated the molybdenum trioxide. Copper substrates of dimensions 10x10x5 mm were polished down to ~ 20 nm of roughness by COMEB. Before the evaporation the substrate was cleaned in 2-Propanol solution and washed using milliQ water.

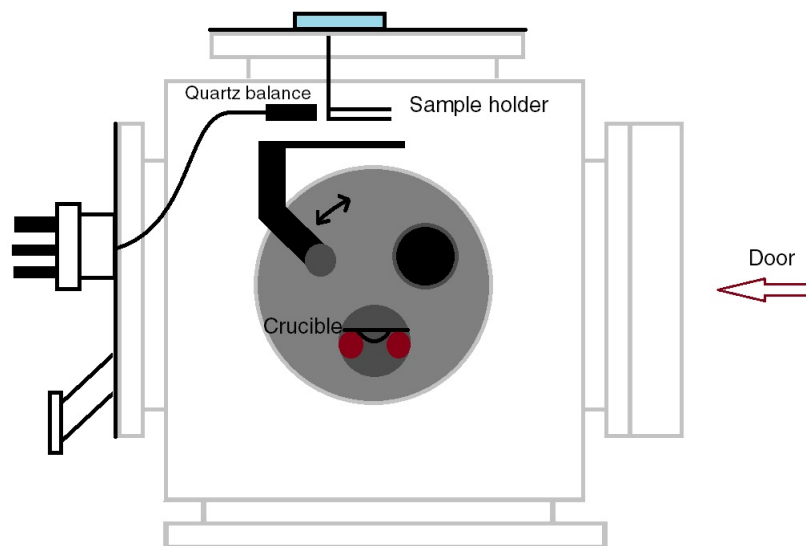


Figure 1: Schematic layout of the evaporation setup inside the HV chamber. On top is placed the sample and the quartz balance. The rotating shutter allows start and stop the evaporation of the oxide from a crucible located at the bottom of the chamber.

The evaporation layout is based on a stainless steel high vacuum (HV) chamber shown in figure 1. Inside the HV chamber a tungsten crucible connected to two copper electrodes allows the evaporation of the molybdenum trioxide at the temperature of 550 °C. The sample holder is placed above the crucible above a slit that allows controlling the flow of the evaporated material using a rotating mask. Deposits are controlled by a quartz crystal microbalance placed next to the sample. After positioning the sample inside the chamber, vacuum pumps are turned on and after 1-2 h the working pressure reach low $\sim 6-10$ mbar. This low pressure is maintained during the evaporation process after the current generator slowly reached the value of 80 A. The duration of the evaporation process is associated to the thickness of the deposition, typically ranging from 5 to 15 minutes. The deposition with the quartz balance has been calibrated with the AFM technique through a measurement of a molybdenum layer of 50 nm deposited on a silicon wafer. The uncertainty in the layer deposition is ~ 1 nm.

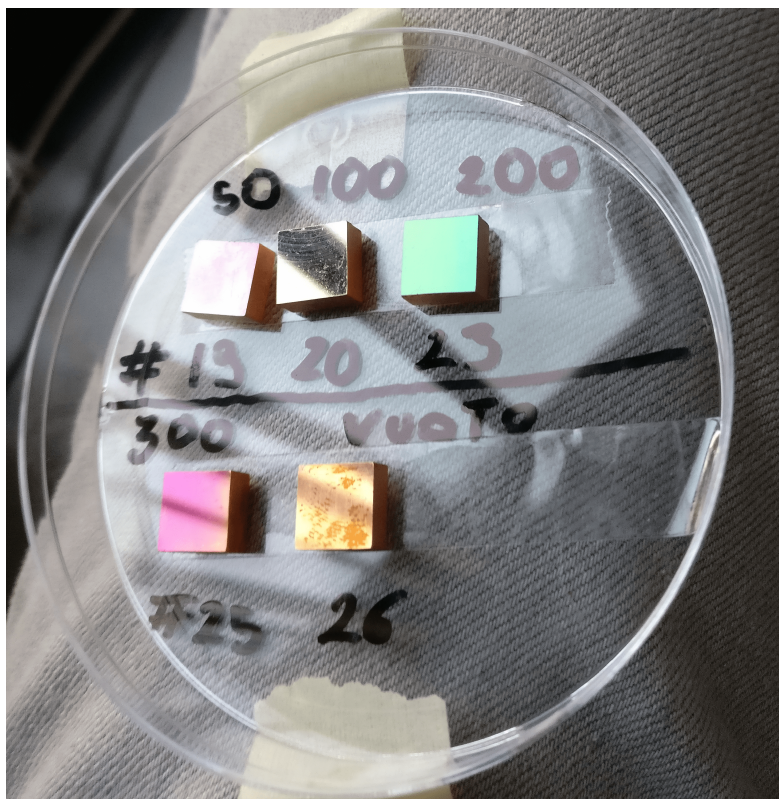


Figure 2: Photograph showing evaporated samples of MoO₃ on copper. Due to the different thickness, each film can be easily recognized by its different colour.

2.1 XRD Characterization

The MoO₃ samples were first characterized by X-Ray Diffraction (XRD) in order to check the presence of ordered crystalline phases. The diffraction experiments were performed at the Frascati National Laboratory (LNF) using a Seifert MZ IV diffractometer with a Cu anode, which operates at 40 kV and 30 mA with a Ni filter. The X ray spot used has

dimensions of 10 mm x 3 mm. Measurements were carried out with a 2θ geometry. As shown in figure 3 the films with 50 nm and 100 nm thickness show only diffraction peaks from the substrate pointing out that the deposited layers contains disordered oxide phases

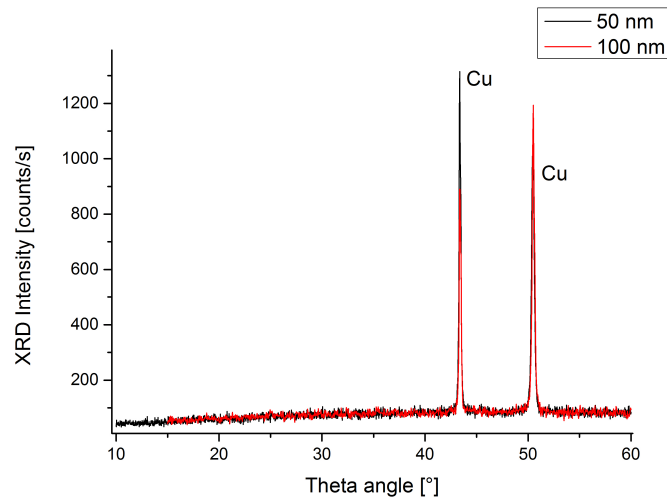


Figure 3: Comparison of the XRD patterns of a 50 nm thick MoO_3 film (black) and a 100 nm film (red). The two peaks measured in these patterns are associated to the diffraction from the copper substrate.

2.2 Experimental Set Up

The MoO_3 samples we measured have a thickness of: 30 nm, 60 nm, 100 nm, 300 nm and 750 nm. The reference copper substrate, i.e., without coating, has been also measured. Samples were located in an optical cryostat, equipped with a cold finger using a temperature controlled liquid helium continuous flow (see Figure 4). The measurements were performed cooling the sample in the temperature range from 300 K to 20 K. The electrical resistance has been recorded by the Agilent 3458A Multimeter, while the temperature was monitored by the Intelligent temperature controller of the Oxford Instruments. The electrical contact has been made as follow: two point contacts made of silver paint were realized on the MoO_3 surface. The resistance error of these measurement is 1% of the reading while that on the temperature is ± 10 mK.

3 Data and Discussion

In this section we report data of the electrical resistance as function of temperature. The electrical resistance of thin films, e.g., with thickness of 30 nm and 60 nm is compared in Figure 5.

The resistance temperature dependence shows a metallic trend and a similar behaviour is showed by the bare copper substrate as reported in the right panel of Figure 6.

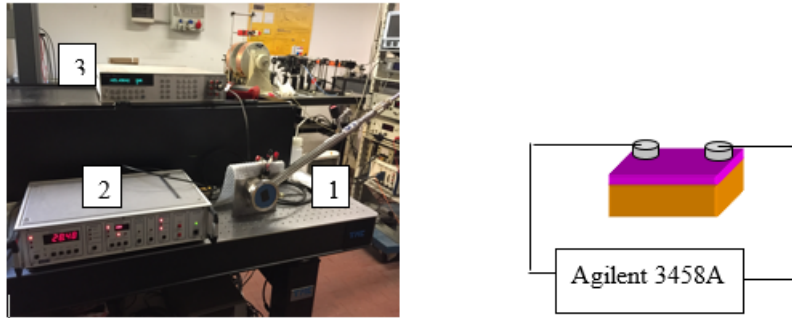


Figure 4: (Left) The experimental setup: 1- the optical cryostat with the cold finger; 2- the Intelligent temperature controller of the Oxford Instruments; 3- the Agilent 3458A Multimeter; (Right) layout of the sample with the two electrodes on the MoO₃ film.

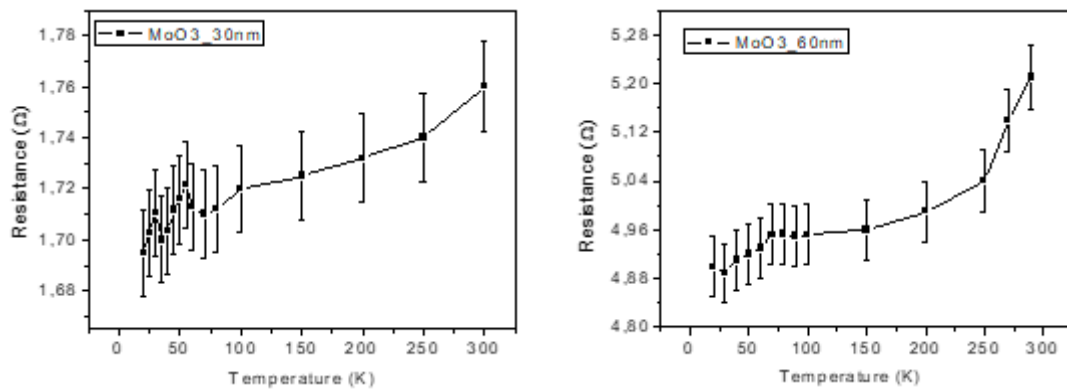


Figure 5: Electrical resistance vs. temperature for MoO₃ samples with thickness: 30 nm (left) and 60 nm (right).

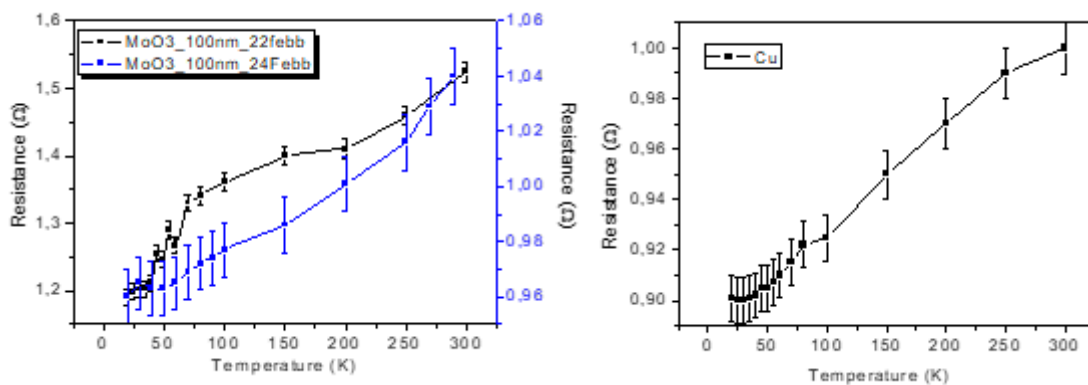


Figure 6: The temperature resistance dependence vs. temperature of the copper substrate (right); electrical resistance vs. temperature for the MoO₃ film 100 nm thick measured in two different days (left). Looking at the resistance scale the trend is quite similar.

The reproducibility of the measurement has been tested for one sample. In figure 6 (right panel) two measurements of the electrical resistance of the 100 nm film of MoO₃ recorded in two different days, are compared. The two trends are quite similar, although

the electrical resistance behaviour of the second run is lower down to the low temperature region (> 40 K). The behaviour observed is due to the percolative characteristic of transport of these heterogeneous disorder films and, in general, the copper electrical resistance is the main contribution.

In figure 7 we compare data of the 300 nm, 500 nm and 750 nm films of MoO₃ on copper. It could be noted that for thickness above 500 nm the temperature electrical resistance dependence of the oxide films show a semiconducting behaviour. Then, the MoO₃ films with thickness of 500 nm and 750 nm show a semiconducting trend while for the 300 nm MoO₃ film the behaviour looks still metallic.

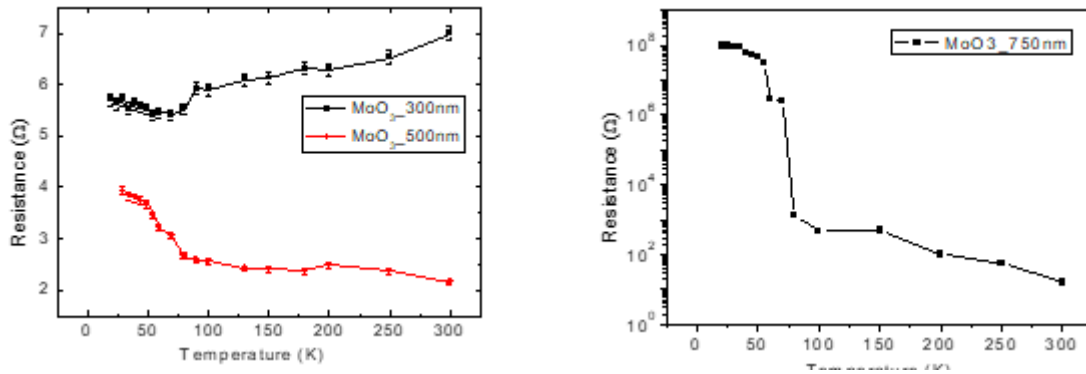


Figure 7: Comparison of the electrical resistance vs. temperature for MoO₃ films with thickness of 300 nm and 500 nm on copper (left); the same using a semilogarithmic scale for the 750 nm thick sample (right) that exhibits a semiconducting behavior with a very high resistance at low temperature (hundreds of MΩ).

In figure 8 we compare the behaviour of films with thickness of 30 nm, 60 nm and 100 nm. Two different Y-axis scales have been used to outline their trends.

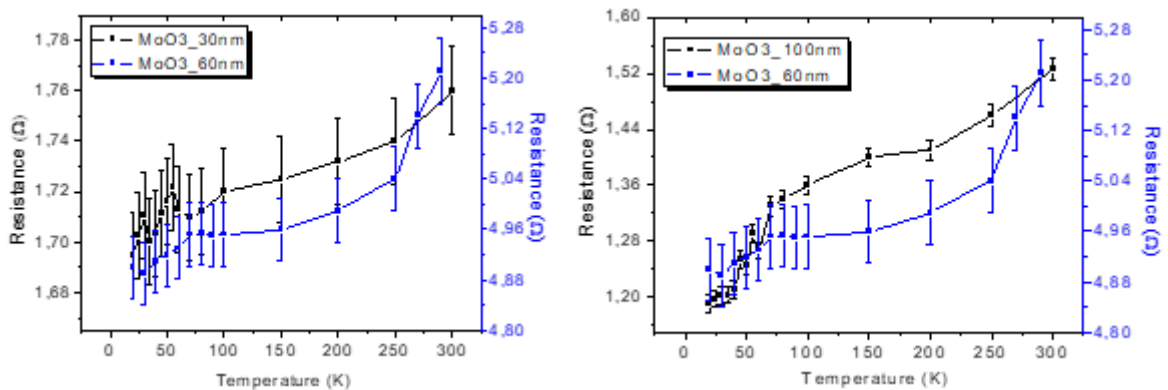


Figure 8: Comparison of the electrical resistance vs. temperature for MoO₃/Cu samples with MoO₃ thickness of 30 nm and 60 nm (left), 60 nm and 100 nm (right). Two Y-axis scale are used, due to the different range of the samples electrical resistance.

In figure 9 the comparison between the electrical resistance vs. temperature for samples with different MoO₃ thickness and copper is reported. In figure 7 (left) is evident

that the electrical resistance of the MoO₃ film 500 nm thick shows a semiconducting behaviour. In figure 9 (right panel) a comparison between all measured films and the copper substrate is reported after normalization of the electrical resistance. In this way the experimental trend is enhanced, and from the comparison is even more evident that for thickness above 500 nm the temperature dependence of the electrical resistance shows a clear semiconducting behaviour.

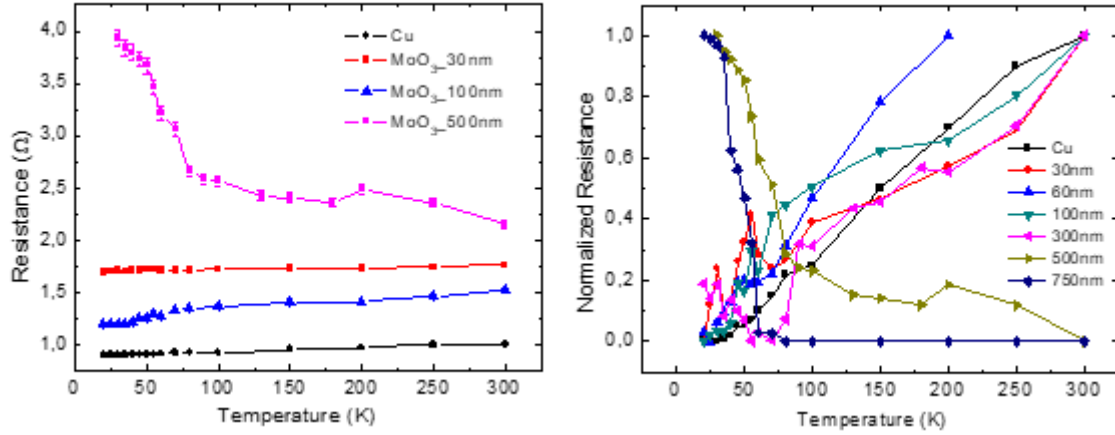


Figure 9: Comparison of the electrical resistance vs. temperature for the Cu substrate, and for MoO₃ films with thickness: 30 nm, 100 nm and 500 nm (left); data of the electrical resistance vs. temperature normalized between 0 to 1 for thickness from 30 nm to 750 nm (right).

In table 1 we list the value of the electrical resistance at 20 K and at room temperature for all measured films. It could be noted that the maximum electrical resistance variation appears in the films with 500 nm and 750 nm, both showing a semiconducting behavior.

Table 1: The electrical resistance of MoO₃ films at low temperature (20 K) and at 290 K. MoO₃ thickness (nm) Electr. res. (Ω) @20K Electr. res. (Ω) @290K Electr. res. variation (Ω) $R_{290K}-R_{20K}$

MoO ₃ thickness (nm)	Electr. res. (Ω) @20K	Electr. res. (Ω) @290K	Electr. res. variation (Ω) $R_{290K}-R_{20K}$
0 (only Cu)	0,901	1	0,099
30	1,69	1,75	0,06
60	4,89	5,21	0,32
100	1,19	1,48	0,29
300	5,70	7	1,30
500	4,30	2,15	2,15
750	9E7	16	9E7

4 Local Morphology and Conduction Properties of Thin Films

Scanning Tunnelling Microscopy (STM) is a useful technique to characterize the surface structure. Due to the limitation of the STM technique to operate on conductive sam-

ples, this preliminary characterization was first restricted to bulk Cu and to the thinnest film of MoO₃ (30 nm) on copper. Experiments were performed using an Omicron-STM (Omicron, Taunusstein, Germany) apparatus, acquiring data with the Omicron software (Omicron Scala Pro). Data were collected in constant current mode at room temperature under ultrahigh vacuum conditions (base pressure 8×10^{-11} mbar) using electrochemically etched tungsten tips (99.9% purity, Goodfellow GmbH, Friedberg, Germany). Some images are showed in figure 10.

Scanning Tunneling Spectroscopy (STS) data (I vs. V curves) were collected simultaneously with image acquisition disabling the feedback loop circuit during the sweep and keeping the tip-sample distance fixed by the set current. The corresponding dI/dV vs. V curves were mathematically evaluated to check the local electronic density of states. Statistical analysis of the collected I-V data and the corresponding derivative curves gave very small error bars (not showed in these figures). In Figure 10 we compare two topographical images obtained at room temperature on two samples, which have not undergone to a cleaning procedure. Images collected on large areas of the bulk Cu sample show that the surface is not flat but irregular with an average roughness of ~ 7.4 nm. The figure 10 (left) obtained on a small area (250 nm x 250 nm) shows that the same surface has a granular structure. This is due to the manufacturing technique and to the presence of some native oxides on the surface. The same behaviour was observed for the thinnest MoO₃ film (30 nm) on copper. For this sample the roughness drops to ~ 4 nm. The decrease is probably due to a levelling effect. The trend can be better appreciated in figure 10 (right panel) where a granular structures, but a slightly smoother surface, can be recognized.

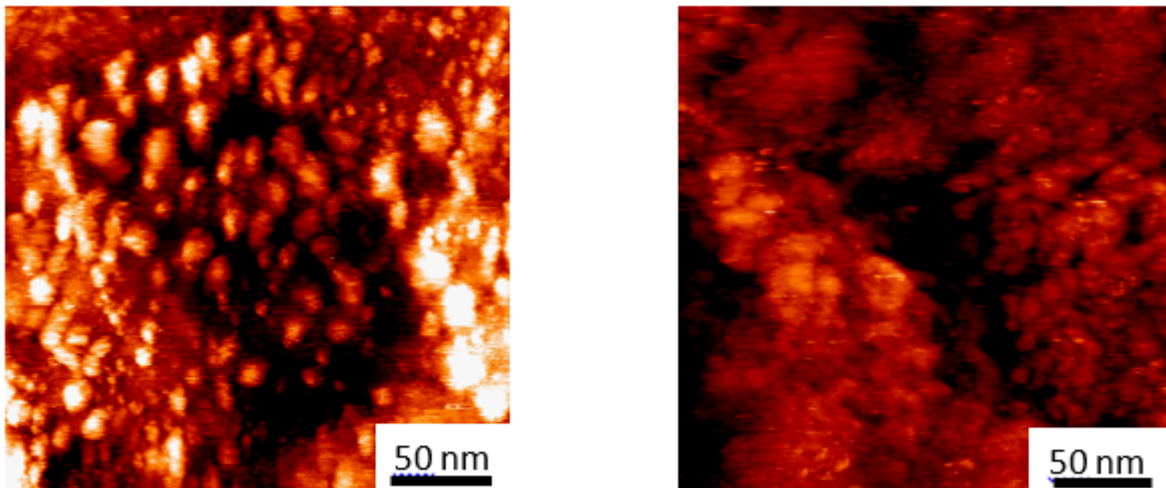


Figure 10: STM images obtained on bulk Cu (left) and Cu with a 30 nm oxide layer (right). The scan areas are 250 nm x 250 nm (bar 50 nm). The bulk Cu surface has a marked granular structure partially reduced after the oxide deposition. Tunneling conditions: bulk Cu $I_t = 0.5$ nA, $V_b = 1.5$ Volt; Cu-MoO₃ oxide (30 nm) $I_t = 0.3$ nA, $V_b = 4$ Volt)

Local spectroscopy data collected on small sample areas during the topography

acquisition return other interesting information about the local conductivity at room temperature of these films. In Figure 11 we compare the current-voltage curves obtained on the bulk Cu (blue), on a 30 nm molybdenum oxide films (red) and the related calculated derivative dI/dV vs. V . Figure 11 (left) clearly shows that the bulk Cu (blue line) current response is linear and almost symmetric (for both positive and negative applied bias) in all the voltage ranges investigated, again pointing out a clear metallic behaviour. By contrast, for the Cu sample (red line) covered by a thin oxide layer the current is very low compared to that of the Cu bulk and, is different from zero only for an applied voltage ≥ 2 V. This trend is better seen in the magnified views of the curves around (-1;+1) V. In particular, we estimated for the Cu-oxide sample a gap of $\sim 2.4 \pm 0.2$ eV. The calculated first order derivative of the I-V curves contains other useful information regarding the local density of states of our samples. Figure 11 (top right) shows that the Cu bulk has a density of states different from zero in all ranges studied with two maxima around ± 3.8 eV. At variance, the Cu-oxide (30 nm) film has no states available around (-1;+1) V, but around ± 4.8 eV exhibits two symmetric maxima that could be associated to local states available for the electron transport. The analysis of the observed behaviours is still in progress.

5 Infrared Measurements

Finally we performed normal incidence reflectance spectroscopy in the mid-infrared (500-8000 cm^{-1}) at room temperature through a Hyperion 1000 microscope coupled with a Vector 22 Bruker spectrometer. The reflectance has been calculated through the ratio between the reflected intensity by the MoO_3 film over that reflected by a clean Cu surface. Several points have been measured by obtaining the same results. In Fig. 12 we compare the reflectance spectra of two samples: one with a thickness of 30 nm (red) and a second one 300 nm thick (black).

The thinner film shows a reflectance lower than one in the entire spectral region. A well evident minimum appears around 3500 cm^{-1} . This minimum can be associated to the plasma edge of MoO_3 , confirming the metallic response of thin films of MoO_3 . A broad bump is also present around 7000 cm^{-1} , possibly associated to an interband transition. Some vibrational modes are also present below 1000 cm^{-1} . By increasing the thickness (300 nm, black curve), the reflectance becomes nearly flat. This is a strong indication that this film shows an insulating response acting, practically, as an antireflectance coating of the Cu crystal.

6 Conclusion

Transport measurements have been performed on several films of MoO_3 deposited on bulk Cu substrate Cu with a thickness of 5 nm. Films with thickness ranging from 30 nm to 300 nm showed a decreasing of the electrical resistance at low temperature. The

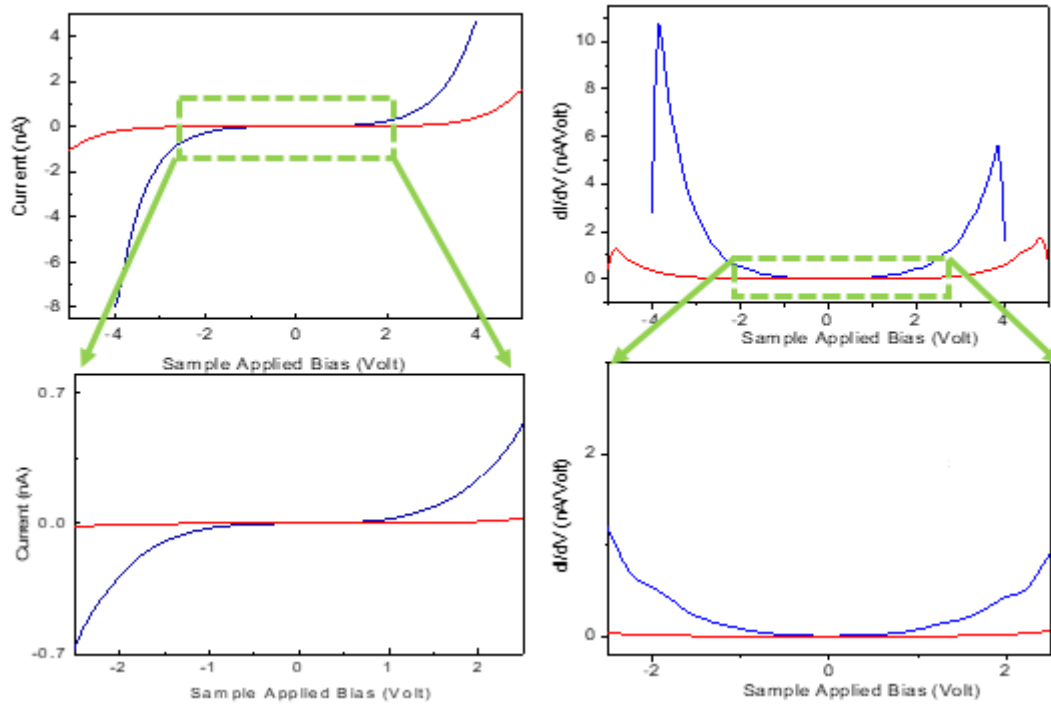


Figure 11: Spectroscopy data of the bulk Cu (blue) and of the Cu-MoO₃ (30 nm) sample (red) collected with an applied bias of (-5;+5) V. Upper left: the I-V curve for bulk Cu showing the metallic behaviour while for the Cu-oxide the current is lower and shows an insulating response between (-1;+1) V, as outlined by the zoom in the bottom left part of the image. Upper right: the evaluated derivative of the I-V curves confirms that the bulk Cu has available empty states in all the voltage range studied with two symmetric maxima located around 3.8 eV, while no states are available around ± 1 V. In the Cu-oxide sample two symmetric maxima appear around 4.8 eV.

thinnest MoO₃ film (30 nm) shows also a lower resistance variation compared to thicker films of 60 nm and 100 nm. Moreover, the thickest MoO₃ layers of 500 nm and 750 nm show a semiconducting behaviour. Then, increasing the MoO₃ thickness it is clear that the electrical resistance vs. temperature increases and the metallic behaviour observed for the thin films has to be associated to the underlying metallic substrate. To improve the sensitivity to the electrical resistance variation of these thin coatings and to ensure a good thermal coupling between the MoO₃ layer and the cryostat cold finger, we are planning to grow other MoO₃ films on a much thinner Cu substrate, i.e., with a maximum thickness of 1-2 nm.

Acknowledgments

We kindly acknowledge Comeb S.r.l. for the manufacture of the copper substrates at low roughness. A special thanks is devoted to G. Cappuccio for his support to diffraction experiments performed in the X-Lab at Frascati.

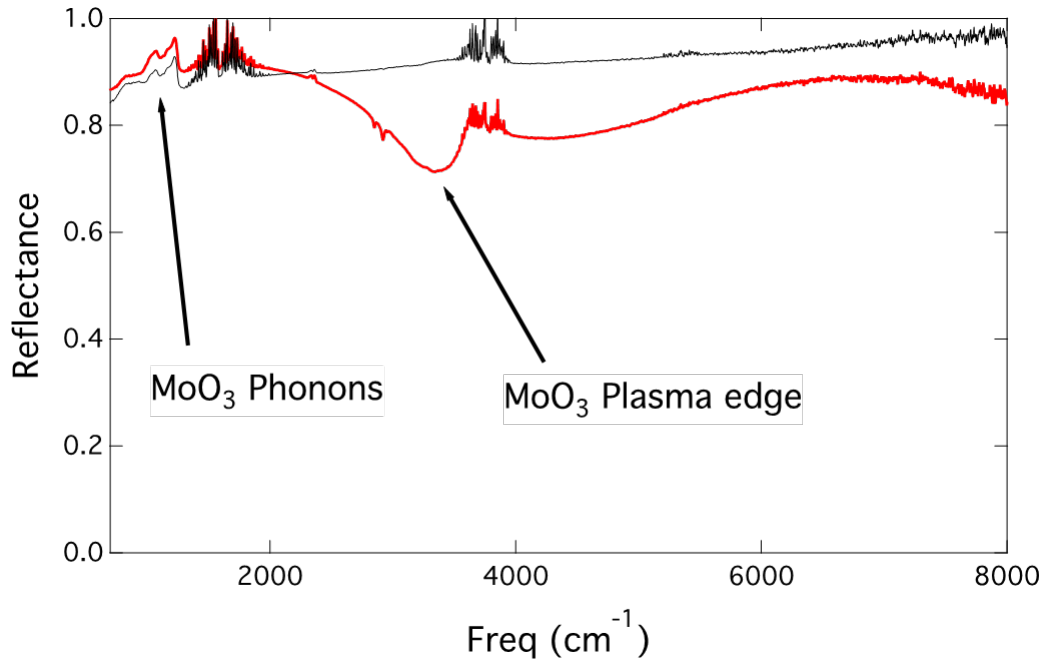


Figure 12: Comparison of the absolute reflectance of MoO₃ films of 30 and 300 nm thickness. While the thinner film shows, at room temperature, a metallic behaviour with a well evident plasma edge in the mid-infrared region, the 300 nm thick film shows an insulating behaviour with a flat (<1) reflectance. The narrow peaks around 1600 and 3900 cm⁻¹ are due to the water vapour absorption in the spectrometer.

References

- [1] M.T. Greiner, L. Chai, M.G. Helander, Wing-Man Tang and Zheng-Hong Lu, *Adv. Funct. Mater.* 23 (2013) 215–226
- [2] S. Lagotzky, R. Barday, A. Jankowiak, T. Kamps, C. Klimm, J. Knobloch, G. Müller, B. Senkovskiy and F. Siewert, *Eur. Phys. J. Appl. Phys.* 70 (2015) 21301-p8
- [3] A. Marcelli, B. Spataro, S. Sarti, V.A. Dolgashev, S. Tantawi, D.A. Yeremian, Y. Higashi, R. Parodi, A. Notargiacomo, J. Xu, G. Cappuccio, G. Gatti, G. Cibin, *Surf. Coat. Tech.* 261 (2015) 391-397
- [4] A. Marcelli, B. Spataro, G. Castorina, W. Xu, S. Sarti, F. Monforte, G. Cibin, *Condensed Matter* 2 (2017) 18; doi:10.3390/condmat2020018